This article has been accepted for publication in IEEE Wireless Communications Letters. This is the author's version which has not been fully edited and content may change prior to final publication. Citation information: DOI 10.1109/LWC.2026.3703877

Generalized Least Squares Based Covariance Reconstruction for DoA Estimation with Hybrid Partially Connected Arrays

Miguel Rivas-Costa and Carlos Mosquera

atlanTTic Research Center, Universidade de Vigo, Vigo, Spain
{mrivascosta,mosquera}@gts.uvigo.es

***Abstract*—Accurate Direction of Arrival (DoA) estimation with Partially-Connected (PC) arrays is hindered by dimensionality compression in the analog domain. This loss of spatial information restricts the degrees of freedom (DoF) available, degrading the performance of high-resolution algorithms. To recover the lost DoFs, we propose an approach that reconstructs the equivalent spatial covariance matrix (SCM) of the fully digital array. The method leverages the discrete Short-Time Fourier Transform (STFT) underlying the PC measurements, and formulates SCM reconstruction as a Generalized Least Squares (GLS) estimation problem. The resulting estimator, asymptotically efficient, is validated across multiple scenarios with numerical results.**

***Index Terms*—Direction of arrival estimation, hybrid analog and digital arrays, covariance matrix reconstruction, array signal processing.**

I. Introduction

Accurate estimation of the Direction of Arrival (DoA) is fundamental for next-generation 6G MIMO, radar, and satellite communications [1], [2]. To mitigate the prohibitive cost of Fully Digital (FD) arrays, which require a dedicated radio frequency (RF) chain per antenna, Hybrid Analog-Digital (HAD) architectures [3] and emerging paradigms such as Fluid Antennas [4] have gained significant traction. While Fully-Connected (FC) HAD arrays offer maximum beamforming flexibility, Partially-Connected (PC) HAD architectures provide a more hardware-efficient implementation by mapping disjoint antenna sub-arrays to a limited number of RF chains, significantly reducing the number of phase-shifters [3]. To further minimize hardware, passive beamforming networks such as the Rotman lens replace active components with passive analog devices to drastically reduce power consumption and cost [5]. However, this efficiency comes at the cost of reduced flexibility, as the analog beamforming is limited to Discrete Fourier Transform (DFT) configurations.

However, since the number of RF chains is generally much lower than the number of antenna elements, HAD architectures reduce the degrees of freedom (DoF) required for high-resolution subspace algorithms like MUSIC, which rely on the Spatial Covariance Matrix (SCM) of the FD array [6]. Furthermore, HAD architectures require a codebook of analog beamforming configurations. Minimizing the size of the codebook is critical to reducing the sensing time, which requires analytical parameterization to avoid losing vital spatial information. Works as [7] or [8] propose techniques for estimating the SCM with a single RF-chain using DFT beamforming, the latter also extended to FC [9] and PC [10] architectures, respectively. These contributions lack a statistical characterization of the estimation process, leaving room for further improvements.

In our previous work [11], [12], we addressed the FC scenario, demonstrating that the estimation process can be significantly improved while reducing the size of the codebook by exploiting inter-RF-chain correlations and the specific statistics of measurement errors. Also for the FC case, a convenient parameterization of the sensing codebook is developed in [13], leading to the application of an asymptotically efficient Generalized Least Squares (GLS) estimator, although the results cannot be transferred to PC arrays, which are usually preferred in practical applications for hardware complexity, power consumption and scalability reasons.

In this paper, we derive a GLS estimator for the SCM of the FD array by explicitly exploiting the inter-sub-array output correlations of PC arrays, formulated through a discrete Short Time Fourier Transform (STFT). The proposed approach improves the performance of DoA estimation with independent sub-arrays, when used in conjunction with high-resolution subspace methods.

Notation: Throughout this paper, upper- and lower-case boldface letters denote matrices and vector, respectively. The entry in the uth row and the vth column of the matrix $\boldsymbol{A}$ is denoted by $\boldsymbol{A}[u, v]$, and the uth element of the vector $\boldsymbol{a}$ is denoted by $\boldsymbol{a}[u]$. The operations $(\cdot)^*, (\cdot)^T$ and $(\cdot)^H$ represent the complex conjugate, transpose and Hermitian transpose. $\otimes$ denotes the Kronecker product. The $N \times N$ identity matrix is denoted by $\boldsymbol{I}_N$, while $\mathbf{0}_{M,N}$ represents an $M \times N$ matrix of zeros. The operators $|\cdot|$, $\|\cdot\|_2$ and $\mathbb{E}[\cdot]$ represent the absolute value, the ℓ_2-norm and the expectation, respectively. The operator $\mathrm{vec}(\boldsymbol{A})$ refers to the vectorization of the matrix $\boldsymbol{A}$, formed by stacking its columns into a single vector. A block-diagonal matrix with constituent blocks $\boldsymbol{A}_0, \ldots, \boldsymbol{A}_{N-1}$

This research was funded in part by MICIU/AEI/10.13039/501100011033 FEDER/EU under projects PID2021-122483OA-I00 and PID2022-136512OB-C22. Work supported in part by the Xunta de Galicia (Secretaría Xeral de Universidades) under a Predoctoral Scholarship (cofunded by the European Social Fund) ED481A 2022/407.

This article has been accepted for publication in IEEE Wireless Communications Letters. This is the author's version which has not been fully edited and content may change prior to final publication. Citation information: DOI 10.1109/LWC.2026.3703877

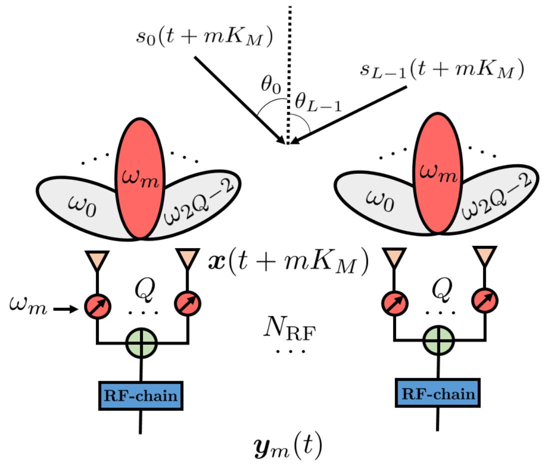

Fig. 1: Geometry of the problem. ULA with N antennas, N_{RF} RF chains, and L impinging sources.

is denoted by blk diag$(\boldsymbol{A}_0, \ldots, \boldsymbol{A}_{N-1})$.

II. Signal model

We assume L uncorrelated narrowband sources impinging on a Partially-Connected (PC) hybrid analog and digital array with N antennas and N_{RF} sub-arrays, each connected to an independent RF-chain (Fig. 1). The number of antennas per sub-array is Q, with $N = Q \cdot N_{\text{RF}}$, and constant inter-element distance equal to $d = \lambda/2$ for wavelength λ. Each sub-array is equipped with an analog combiner formed by Q phase-shifters and constant amplitudes.

We assume K time snapshots distributed in M batches, during which the phase-shifter configuration remains constant, changing after a time window of $K_M = K/M$ snapshots. Following downconversion and sampling, the signal $x(t)$ goes through the analog beamforming in the mth batch as

$$\begin{aligned}\boldsymbol{y}_m(t) &= \boldsymbol{B}_m^H \boldsymbol{x}(t+mK_M)\\ &= \boldsymbol{B}_m^H(\boldsymbol{A}(\boldsymbol{\psi})\boldsymbol{s}(t+mK_M) + \boldsymbol{n}(t+mK_M)), \qquad (1)\end{aligned}$$

for $0 \leq m < M$ and $0 \leq t < K_M$. Here, $\boldsymbol{s}(t) = [s_0(t), \ldots, s_{L-1}(t)]^T$ is the transmitted source vector, modeled as a zero mean, random vector with covariance $\boldsymbol{R}_s = \text{diag}(\sigma_{s,0}^2, \ldots, \sigma_{s,L-1}^2)$. Noise is a complex white Gaussian random vector $\boldsymbol{n}(t) \in \mathbb{C}^{N\times 1}$ with zero mean and a covariance matrix $\sigma_n^2 \boldsymbol{I}_N$. The matrix $\boldsymbol{A}(\boldsymbol{\psi}) = [\boldsymbol{a}(\psi_0), \ldots, \boldsymbol{a}(\psi_{L-1})] \in \mathbb{C}^{N\times L}$, named the array manifold, encodes the DoA information; its ℓth column is the steering vector of the ℓth source expressed by $\boldsymbol{a}(\psi_\ell) = [1, \ldots, e^{j(N-1)\psi_\ell}]^T$ for a perfectly calibrated array, with the directional sine $\psi_\ell \triangleq \pi\sin(\theta_\ell)$.

The set of beamforming matrices $\{\boldsymbol{B}_m \in \mathbb{C}^{N\times N_{\text{RF}}}\}$ is referred to as the *codebook* of the PC-HAD array, and such that each $\boldsymbol{B}_m$ follows a block diagonal structure

$$\boldsymbol{B}_m = \text{blk diag}\left(\boldsymbol{b}_{m,0} \quad \ldots \quad \boldsymbol{b}_{m,N_{\text{RF}}-1}\right), \qquad (2)$$

where $\boldsymbol{b}_{m,n} \in \mathbb{C}^{Q\times 1}$ is the beamforming vector of the nth sub-array in the mth batch. For Fourier beamforming, we synthesize beams pointing at spatial frequencies (or directional sines) $\omega_{m,n}$:

$$\boldsymbol{b}_{m,n}[q] = Q^{-1/2} e^{j\omega_{m,n} q} \quad 0 \leq q < Q. \qquad (3)$$

After beamforming, the received signal $\boldsymbol{y}_m \in \mathbb{C}^{N_{\text{RF}}\times 1}$ is still zero mean with SCM $\boldsymbol{S}_m \in \mathbb{C}^{N_{\text{RF}}\times N_{\text{RF}}}$:

$$\boldsymbol{S}_m \triangleq \mathbb{E}[\boldsymbol{y}_m(t)\boldsymbol{y}_m^H(t)] = \boldsymbol{B}_m^H \boldsymbol{R}_x \boldsymbol{B}_m, \qquad (4)$$

where $\boldsymbol{R}_x \triangleq \mathbb{E}[\boldsymbol{x}(t)\boldsymbol{x}^H(t)]$ is the SCM of the equivalent FD array given by $\boldsymbol{R}_x = \boldsymbol{A}(\boldsymbol{\psi})\boldsymbol{R}_s\boldsymbol{A}^H(\boldsymbol{\psi}) + \sigma_n^2\boldsymbol{I}_N$. Since $\boldsymbol{R}_s$ is diagonal, the SCM is Hermitian Toeplitz and it can be entirely characterized by the $2N-1$ entries of the spatial covariance sequence $\boldsymbol{r}_x \in \mathbb{C}^{(2N-1)\times 1}$, such that

$$\boldsymbol{r}_x[k] \triangleq \boldsymbol{R}_x[k, 0], \quad \boldsymbol{r}_x[-k] = \boldsymbol{r}_x^*[k], \quad 0 \leq k < N. \qquad (5)$$

III. GLS estimation of the SCM

In this section, we develop a GLS framework to estimate the covariance vector $\boldsymbol{r}_x$, without assuming any prior knowledge about the number of sources or the powers involved. The underlying discrete STFT formulation of the PC measurements will be exploited to establish a formal linear mapping between batch covariance matrices $\{\boldsymbol{S}_m\}$ and the sequence $\boldsymbol{r}_x$, ultimately leading to an optimal estimate of $\boldsymbol{r}_x$.

A. STFT Driven Codebook Design

Let $\boldsymbol{S}_m[u,v] = \boldsymbol{B}_m^H[:,u]\boldsymbol{R}_x\boldsymbol{B}_m[:,v]$ be the covariance between outputs of sub-arrays $0 \leq u, v < N_{\text{RF}}$. Given the block diagonal structure of $\boldsymbol{B}_m$ in (2), the uth column only contains non-zero entries for the uth sub-array. Mapping global indices to local ones via $p = uQ + p'$ and $q = vQ + q'$, where $0 \leq p', q' < Q$, the beamformer entries become $\boldsymbol{B}_m[uQ+p', u] = Q^{-1/2}e^{j\omega_{m,u}p'}$. Invoking the Hermitian Toeplitz property $\boldsymbol{R}_x[p,q] = \boldsymbol{r}_x[p-q]$ [7] and defining the phase difference $\Delta\omega_{u,v} \triangleq \omega_{m,u} - \omega_{m,v}$, the covariance matrix simplifies as:

$$\begin{aligned}\boldsymbol{S}_m[u,v] &= Q^{-1}\sum_{p',q'} \boldsymbol{r}_x[p'-q'+(u-v)Q]e^{-j(\omega_{m,u}p' - \omega_{m,u}q')}\\ &= \sum\nolimits_{q=-Q+1}^{Q-1} \boldsymbol{w}(\Delta\omega_{u,v}, q)\boldsymbol{r}_x[q+(u-v)Q]e^{-j\omega_{m,u}q}, \qquad (6)\end{aligned}$$

where the change of variables $q = p' - q'$ collapses the double sum. The weighting function $\boldsymbol{w}(\Delta\omega_{u,v}, q]$ absorbs the remaining inner sum over q' and it is defined as:

$$\boldsymbol{w}(\Delta\omega_{u,v}, q] \triangleq \frac{1}{Q}\sum_{q'=\max(0,-q)}^{\min(Q-1,Q-1-q)} e^{-j\Delta\omega_{u,v}q'}. \qquad (7)$$

Under uniform steering, with all sub-arrays steered toward the same direction, i.e., $\omega_m \triangleq \omega_{m,u}$ $\forall u$ (see Fig. 1), the phase difference is zero, $\Delta\omega_{u,v} = 0$, and a discrete STFT emerges:

$$\boldsymbol{S}_m[u,v] = \sum_{q=-Q+1}^{Q-1}\left(1 - \frac{|q|}{Q}\right)\boldsymbol{r}_x[q+(u-v)Q]e^{-j\omega_m q}. \qquad (8)$$

The entries of $\boldsymbol{S}_m$ are spectral coefficients obtained by partitioning the $2N-1$ samples of the covariance sequence into $2N_{\text{RF}}-1$ overlapping segments of length $2Q-1$, applying a triangular window to each segment, and projecting the result onto the frequency ω_m. Following this path, we design the codebook as a set of $M = 2Q-1$ beamforming matrices. The steering direction for each batch is chosen from a $(2Q-1)$-DFT grid as

$$\omega_m = \frac{2\pi}{2Q-1} m \quad 0 \le m < 2Q-1. \tag{9}$$

Remark 1: The STFT interpretation in (8) provides a unified framework that extends the existing literature to explain the DFT beamforming in PC architectures. In the analog beamforming limit ($N_{\mathrm{RF}} = 1, Q = N, M = 2N-1$), the expression of $S_m \triangleq \boldsymbol{S}_m[0,0]$ matches the result obtained in [7], since (8) provides $2N-1$ samples of the spatial power spectrum:

$$S_m = \sum_{q=-Q+1}^{Q-1} \Big(1 - \frac{|q|}{Q}\Big) \boldsymbol{r}_x[q] e^{-j\omega_m q} \quad 0 \le m < 2N-1.$$

Conversely, for the FD scenario ($N_{\mathrm{RF}} = N, Q = 1, M = 1$), the expression reduces to $\boldsymbol{S}_m[u,v] = \boldsymbol{R}_x[u,v] = \boldsymbol{r}_x[u-v]$, which corresponds to the covariance values of the FD array.

B. GLS Formulation

In practice, the entries of the true batch covariance matrix $\{\boldsymbol{S}_m\}$ are not directly observable. Instead, we rely on estimates, typically computed via the sample average as:

$$\hat{\boldsymbol{S}}_m = K_M^{-1} \sum_{t=0}^{K_M-1} \boldsymbol{y}_m(t) \boldsymbol{y}_m^H(t) \quad 0 \le m < M-1. \tag{10}$$

If we aggregate these measurements into the vector

$$\hat{\boldsymbol{p}} = [\mathrm{vec}(\hat{\boldsymbol{S}}_0)^T, \ldots, \mathrm{vec}(\hat{\boldsymbol{S}}_{M-1})^T]^T, \tag{11}$$

we have that the observation $\hat{\boldsymbol{p}}$ is asymptotically distributed as a complex Gaussian vector [14]–[16][1], with mean

$$\boldsymbol{p}(\boldsymbol{r}_x) \triangleq \mathbb{E}[\hat{\boldsymbol{p}}] = [\mathrm{vec}(\boldsymbol{S}_0)^T, \ldots, \mathrm{vec}(\boldsymbol{S}_{M-1})^T]^T, \tag{12}$$

and block-diagonal covariance matrix defined as

$$\begin{aligned} \boldsymbol{R}_p(\boldsymbol{r}_x) &\triangleq \mathbb{E}[(\hat{\boldsymbol{p}} - \boldsymbol{p}(\boldsymbol{r}_x))(\hat{\boldsymbol{p}} - \boldsymbol{p}(\boldsymbol{r}_x))^H] = \\ &= K_M^{-1} \cdot \text{blk diag}(\boldsymbol{S}_0^T \otimes \boldsymbol{S}_0, \ldots, \boldsymbol{S}_{M-1}^T \otimes \boldsymbol{S}_{M-1}). \end{aligned} \tag{13}$$

Note that while $\boldsymbol{S}_m$ depends on the unknown sequence $\boldsymbol{r}_x$, we omit this dependence for clarity. Consequently, a feasible GLS estimator of the spatial covariance sequence (5) is obtained by solving

$$\hat{\boldsymbol{r}}_x = \arg\min_{\boldsymbol{r}_x} \|\hat{\boldsymbol{R}}_p^{-1/2}(\hat{\boldsymbol{p}} - \boldsymbol{p}(\boldsymbol{r}_x))\|_2^2, \tag{14}$$

where $\hat{\boldsymbol{R}}_p$ is a consistent estimator of $\boldsymbol{R}_p(\boldsymbol{r}_x)$ obtained by replacing $\{\boldsymbol{S}_m\}$ with $\{\hat{\boldsymbol{S}}_m\}$ in (13). Under this consistency, the solution of (14) shares the same asymptotic properties as the GLS estimator which uses the true $\boldsymbol{R}_p(\boldsymbol{r}_x)$ [17].

The solution to (14) can exploit the linear mapping between the covariance sequence $\boldsymbol{r}_x$ and the vector $\boldsymbol{p}(\boldsymbol{r}_x)$ through (8) and (12). Specifically, since each $\boldsymbol{S}_m$ is Hermitian Toeplitz, it is uniquely determined by only $2N_{\mathrm{RF}}-1$ entries. By combining this property with the spectral representation of the entries $\boldsymbol{S}_m[u,v]$, we can decompose the vectorized matrix $\mathrm{vec}(\boldsymbol{S}_m)$ into a cascade of linear operators:

$$\begin{aligned} \mathrm{vec}(\boldsymbol{S}_m) &= \boldsymbol{S}_m[0,0]\mathrm{vec}(\boldsymbol{D}_0) + \\ &+ \sum_{n=1}^{N_{\mathrm{RF}}-1} \Big(\boldsymbol{S}_m[n,0]\mathrm{vec}(\boldsymbol{D}_n^T) + \boldsymbol{S}_m[0,n]\mathrm{vec}(\boldsymbol{D}_n)\Big) \\ &= \boldsymbol{\Sigma}_T \boldsymbol{P}_{f,m} (\boldsymbol{I}_{2N_{\mathrm{RF}}-1} \otimes \boldsymbol{\Omega}) \boldsymbol{P}_s \boldsymbol{r}_x, \end{aligned} \tag{15}$$

where $\{\boldsymbol{D}_n \in \{0,1\}^{N_{\mathrm{RF}} \times N_{\mathrm{RF}}}\}$ are basis matrices defined as $\boldsymbol{D}_n[u,v] = 1$ if $v - u = n$ and zeros otherwise. This decomposition decouples the measurement process into a spatial expansion operator $\boldsymbol{P}_s$:

$$\boldsymbol{P}_s = [\boldsymbol{P}_{s,0}^T, \ldots, \boldsymbol{P}_{s,2N_{\mathrm{RF}}-2}^T]^T, \tag{16}$$

$$\boldsymbol{P}_{s,n} = [\boldsymbol{0}_{(2Q-1),nQ}, \boldsymbol{I}_{2Q-1}, \boldsymbol{0}_{(2Q-1),2(N-Q)-nQ}], \tag{17}$$

followed by a $2N_{\mathrm{RF}}-1$ windowed DFT $(\boldsymbol{I}_{2N_{\mathrm{RF}}-1} \otimes \boldsymbol{\Omega})$ with

$$\boldsymbol{\Omega}[u,q] = (1 - |q|/Q) e^{-j\frac{2\pi}{2Q-1}uq}, \tag{18}$$

for $0 \le u < 2Q$ and $-Q < q < Q$. The spectral selector $\boldsymbol{P}_{f,m}$ selects the spectral coefficients in the mth batch as

$$\boldsymbol{P}_{f,m} = \boldsymbol{I}_{2N_{\mathrm{RF}}-1} \otimes \boldsymbol{e}_m^T, \tag{19}$$

where $\boldsymbol{e}_m \in \{0,1\}^{(2Q-1)\times 1}$ is defined such that $\boldsymbol{e}_m[m] = 1$ and zeros elsewhere. The final Hermitian Toeplitz operator maps the selected spectral coefficients into the vectorized matrix $\mathrm{vec}(\boldsymbol{S}_m)$ via

$$\boldsymbol{\Sigma}_T = [\mathrm{vec}(\mathbf{D}_{N_{\mathrm{RF}}-1}), \ldots, \mathrm{vec}(\mathbf{D}_0), \ldots, \mathrm{vec}(\mathbf{D}_{N_{\mathrm{RF}}-1}^T)]. \tag{20}$$

Thus, the aggregated vector $\boldsymbol{p}(\boldsymbol{r}_x)$ in (12) can be expressed as

$$\boldsymbol{p}(\boldsymbol{r}_x) = (\boldsymbol{I}_M \otimes \boldsymbol{\Sigma}_T) \boldsymbol{P}_f (\boldsymbol{I}_{2N_{\mathrm{RF}}-1} \otimes \boldsymbol{\Omega}) \boldsymbol{P}_s \boldsymbol{r}_x = \boldsymbol{\Psi} \boldsymbol{r}_x, \tag{21}$$

with all the scanned spatial frequencies grouped into the codebook matrix $\boldsymbol{P}_f = [\boldsymbol{P}_{f,0}^T, \ldots, \boldsymbol{P}_{f,M-1}^T]^T$. Substituting (21) into the optimization problem (14), the GLS solution reduces to a closed-form estimator:

$$\hat{\boldsymbol{r}}_x = (\boldsymbol{\Psi}^H \hat{\boldsymbol{R}}_p^{-1} \boldsymbol{\Psi})^{-1} \boldsymbol{\Psi}^H \hat{\boldsymbol{R}}_p^{-1} \hat{\boldsymbol{p}}. \tag{22}$$

The overall computational complexity of the proposed method is $\mathcal{O}(N^3)$. Although the estimator involves multiple matrix multiplications, the block-diagonal structure of $\hat{\boldsymbol{R}}_p$ allows for highly efficient evaluation via batch-level processing. The complexity of the product $\boldsymbol{\Psi}^H \hat{\boldsymbol{R}}_p^{-1} \boldsymbol{\Psi}$ is dominated by M independent batch-level multiplications of the form $\boldsymbol{\Sigma}_T^H (\hat{\boldsymbol{S}}_m^{-T} \otimes \hat{\boldsymbol{S}}_m^{-1}) \boldsymbol{\Sigma}_T$. These terms can be efficiently computed using the techniques developed in [15], which avoid the explicit formation of high-dimensional Kronecker products and significantly reduce the computational complexity. However, the algorithm ultimately requires the inversion of the matrix $(\boldsymbol{\Psi}^H \hat{\boldsymbol{R}}_p^{-1} \boldsymbol{\Psi})$, which entails a complexity of $\mathcal{O}(N^3)$ and constitutes the dominant computational bottleneck.

The estimator $\hat{\boldsymbol{r}}_x$ is uniquely determined if $(\boldsymbol{\Psi}^H \hat{\boldsymbol{R}}_p^{-1} \boldsymbol{\Psi})$ in (22) is invertible. If the sample averages $\{\hat{\boldsymbol{S}}_m\}$ in (10) are computed using $K_M \ge N_{\mathrm{RF}}$ snapshots, then $\hat{\boldsymbol{R}}_p$ is positive definite, and invertibility is equivalent to $\boldsymbol{\Psi}$ being full column

[1] While [16] offers a method for HAD architectures, it employs a general model that does not exploit the specific hardware structure for direct covariance estimation. This leads to a multi-dimensional optimization problem with prohibitive computational complexity, making the technique suitable only when the number of sources and their approximate locations are known *a priori*.

rank, i.e., $\text{rank}(\boldsymbol{\Psi}) = 2N - 1$.

Lemma 1. *The matrix* $\boldsymbol{\Psi} = (\boldsymbol{I}_M \otimes \boldsymbol{\Sigma}_T)\boldsymbol{P}_f(\boldsymbol{I}_{2N_{RF}-1} \otimes \boldsymbol{\Omega})\boldsymbol{P}_s$ *has full column rank, i.e., rank*$(\boldsymbol{\Psi}) = 2N-1$*, if the codebook size satisfies* $M \geq 2Q - 1$*.*

Proof. We rely on two rank properties: $\text{rank}(\boldsymbol{A} \otimes \boldsymbol{B}) = \text{rank}(\boldsymbol{A}) \cdot \text{rank}(\boldsymbol{B})$, and $\text{rank}(\boldsymbol{AB}) = \text{rank}(\boldsymbol{B})$ for any full-column rank matrix $\boldsymbol{A}$ [18]. By applying the properties, we preserve the full column rank of $\boldsymbol{\Psi}$ if each constituent matrix has full column rank: *(i)* The columns of $\boldsymbol{\Sigma}_T$ in (20) are formed by vectorized matrices $\text{vec}(\boldsymbol{D}_n)$ that select disjoint matrix diagonals. As these diagonals do not overlap, the columns are mutually orthogonal ($\text{vec}(\boldsymbol{D}_n)^H\text{vec}(\boldsymbol{D}_{n'}) = \text{trace}(\boldsymbol{D}_n^H\boldsymbol{D}_{n'}) = 0$ for $n \neq n'$), giving $\boldsymbol{\Sigma}_T$ full column rank. *(ii)* For $M = 2Q - 1$, $\boldsymbol{P}_f$ in (19) is a square permutation matrix, hence invertible. For $M > 2Q - 1$, $\boldsymbol{P}_f$ retains this submatrix preserving full column rank. *(iii)* $\boldsymbol{\Omega}$ in (18) is square and full-rank because it factors in invertible matrices as $\boldsymbol{\Omega} = (2Q-1)\boldsymbol{FW}$, where $\boldsymbol{F}$ is a $(2Q-1)$-point DFT matrix and $\boldsymbol{W}$ is a diagonal matrix with strictly positive weights: $\{1 - |q|/Q\}_{q=-Q+1}^{Q-1}$. *(iv)* By definition, $\boldsymbol{P}_s$ in (16) is formed via shifted identities with disjoint columns, yielding a full column rank of $2N-1$. Consequently, the full rank of $\boldsymbol{P}_s$ propagates through the product, yielding $\text{rank}(\boldsymbol{\Psi}) = 2N - 1$. □

IV. Simulations

We validate our proposal via $\text{MC} = 2 \cdot 10^3$ independent Monte Carlo realizations. The transmitted signal vector $\boldsymbol{s}(t)$ is complex Gaussian distributed, with normalized power per source such that $\sigma_{s,\ell}^2 = 1 \;\forall \ell$; thus, the signal-to-noise ratio is defined with respect to the noise power: $\text{SNR} = -10\log(\sigma_n^2)$ [dB]. Performance is evaluated via the Root Mean Square Error: $\text{RMSE} = \sqrt{\frac{1}{\text{MC}\cdot L}\sum_{\ell=0}^{L-1}\sum_{i=0}^{\text{MC}-1}(\theta_\ell - \hat{\theta}_{i,\ell})}$, where $\{\theta_\ell\}$ is the true ℓth source DoA and $\{\hat{\theta}_{i,\ell}\}$ is the corresponding estimate in the ith realization. DoAs are estimated by applying the Root-MUSIC algorithm [1] to the reconstructed covariance matrix $\hat{\boldsymbol{R}}_x$. Theoretical limits are provided by the averaged Root Cramer-Rao lower bound (RCRB): $\text{RCRB} = \sqrt{\frac{1}{L}\sum_{\ell=0}^{L-1}\text{CRB}(\theta_\ell)}$, where the expression of $\text{CRB}(\theta_\ell)$ can be found in [16].

We compare our proposal against three baseline schemes suited to the PC architecture: *(i)* (BSA) [10], which employs DFT-based uniform steering but yields suboptimal performance by neglecting the required statistical weighting; *(ii)* Dynamic Covariance Orthogonal Matching Pursuit (DCOMP) [19], which relies on K distinct pseudo-random beamforming matrices[2]; and GramNet [20], a deep-learning-based covariance estimator adapted from switch-based architectures to partially-connected using proposed uniform steering; *(iv)* for $N_{\text{RF}} = N$, the Asymptotic Maximum Likelihood (AML)[3] [15] is used.

[2]In pseudo-random beamforming, the phase of each phase-shifter is drawn from a uniform distribution $\mathcal{U}(0, 2\pi)$.

[3]Note that GLS for FD architectures ($N = N_{\text{RF}}$) is equivalent to AML.

Unlike sparse recovery alternatives [19] that can handle $L \geq N$ sources, our method is limited by the $N-1$ degrees of freedom of the ULA [1]. However, the proposed method effectively overcomes the hardware-constrained scenario $L \geq N_{\text{RF}}$ [21], achieving near-efficient performance as demonstrated in our simulations. To focus on the region of practical interest, the figures display results with $\text{RMSE} \leq 5°$.

First, we evaluate the RMSE of the methods relative to the angular separation between two closely spaced sources, located at $\theta_0 = 0°$ and $\theta_1 = \Delta$. As shown in Fig. 2a the GLS estimator demonstrates rapid convergence to the RCRB as $\Delta \geq 0.87°$ it exhibits a performance close to RCRB for any number of RF chains. Alternatives perform considerably worse in low N_{RF} regimes, whereas our proposal maintains robust performance and converges to the AML benchmark in the FD limit ($N_{\text{RF}} = N$).

The following simulations evaluate the RMSE with $L = 5$ angular closed sources at $\theta_\ell = \{-8°, -2.5°, 0°, 2.5°, 6°\}$. We begin by noting that while DCOMP can achieve an RMSE lower than $1°$ in less congested environments (see Fig. 2a), its performance degrades in the complex scenario analyzed here.

Fig. 2b displays the impact of SNR on estimation accuracy. Specifically, for $N_{\text{RF}} = 2$ we observe a performance plateau at high SNR, behavior caused by a lower or equal number of RF chains than targets, $N_{\text{RF}} < L$, as demonstrated in [21]. Remarkably, for $N_{\text{RF}} = 8$, only our proposal remains close to the RCRB. Finally, in Fig. 2c, we examine the impact of the number of snapshots K. The efficacy of the GLS framework is heavily dependent on the quality of the whitening matrix estimate $\hat{\boldsymbol{R}}_p$. As K increases, the sample covariance matrix $\hat{\boldsymbol{S}}_m$ provides a more consistent estimate of the error statistics, allowing the GLS estimator to weight the measurements more effectively. The simulation confirms that the proposed method approaches the RCRB as samples grows, validating the asymptotic efficiency of the GLS formulation. While asymptotically efficient, the reliance on second-order statistics makes the framework less suited for low-snapshot regimes ($K < 100$) where alternatives, such as sparse recovery techniques or machine learning methods, are typically favored.

V. Conclusion

This work has considered the estimation of the Spatial Covariance Matrix of the equivalent Fully Digital array in PC-HAD architectures by establishing a novel analytical link between analog beamforming and the discrete STFT. This interpretation allowed for the design of a structured codebook that ensures the complete reconstruction of spatial information, effectively bridging the gap in the existent literature between analog beamforming and Fully Digital architectures. The resulting GLS estimator incorporates measurement error statistics to achieve asymptotic efficiency. From the numerical analysis, it was concluded that the framework outperforms other alternatives even in scenarios with a minimal number of RF chains and closely spaced sources. Further work on the

This article has been accepted for publication in IEEE Wireless Communications Letters. This is the author's version which has not been fully edited and content may change prior to final publication. Citation information: DOI 10.1109/LWC.2026.3703877

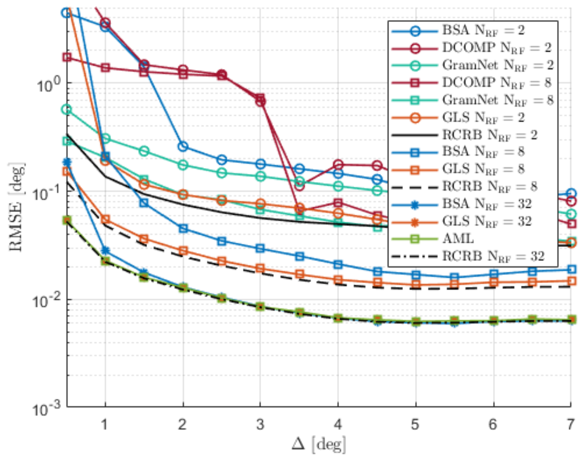

(a)

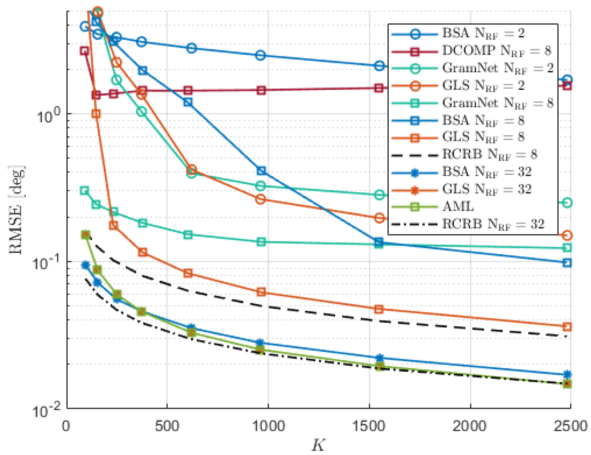

(b)

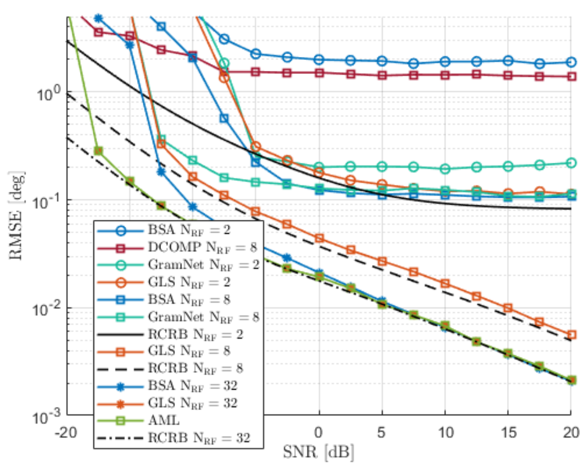

(c)

Fig. 2: $N = 32$ and $N_{\text{RF}} \in \{2, 8, 32\}$. (a) RMSE as a function of angular separation. $\text{SNR} = 0$ dB, $K = 1736$; (b) RMSE as a function of SNR. $\theta_\ell = \{-8^\circ, -2.5^\circ, 0^\circ, 2.5^\circ, 6^\circ\}$, $K = 1736$; (c) RMSE as a function of K. $\theta_\ell = \{-8^\circ, -2.5^\circ, 0^\circ, 2.5^\circ, 6^\circ\}$, $\text{SNR} = 0$ dB.

complexity reduction would be of high interest for practical purposes.

References

[1] H. L. V. Trees, *Optimum Array Processing: Detection, Estimation and Modulation Theory, Part IV*. John Wiley & Sons, 2002.

[2] W. Liu, M. Haardt, M. S. Greco, C. F. Mecklenbräuker, and P. Willett, "Twenty-Five Years of Sensor Array and Multichannel Signal Processing: A review of progress to date and potential research directions," *IEEE Signal Processing Magazine*, vol. 40, no. 4, pp. 80–91, 2023.

[3] A. F. Molisch, V. V. Ratnam, S. Han, Z. Li, S. L. H. Nguyen, L. Li, and K. Haneda, "Hybrid Beamforming for Massive MIMO: A Survey," *IEEE Communications Magazine*, vol. 55, no. 9, pp. 134–141, 2017.

[4] T. Wu, Y. Tian, J. Tang, K. Zhi, M. Elkashlan, K.-F. Tong, N. Al-Dhahir, C.-B. Chae, M. C. Valenti, G. K. Karagiannidis, and K.-M. Luk, "Scalable Fluid Antenna Systems: A New Paradigm for Array Signal Processing," *IEEE Journal of Selected Topics in Signal Processing*, pp. 1–17, 2026.

[5] M. Weiß, M. Kohler, A. Saam, and J. Worms, "Single Snapshot DoA Estimation from a Rotman Lens using Machine Learning Techniques," in *2020 21st International Radar Symposium (IRS)*, pp. 35–39, 2020.

[6] Y. Tian, T. Wu, J. Wu, H. Xu, Y. Shen, X. Lei, and K.-F. Tong, "DOA Estimation for Low-Altitude Networks: HAD Architectures, Methods, and Challenges," 2026. arXiv:2604.00864 [eess.SP].

[7] O. Shmonin, V. Kuptsov, S. Trushkov, K. Ponur, G. Serebryakov, H. Wang, and J. Zhang, "Phase-Independent Beamspace MUSIC Algorithm for a Single Port Phased Antenna Array," in *2023 31st Telecommunications Forum (TELFOR)*, pp. 1–4, 2023.

[8] S. Li, Y. Liu, L. You, W. Wang, H. Duan, and X. Li, "Covariance Matrix Reconstruction for DOA Estimation in Hybrid Massive MIMO Systems," *IEEE Wireless Communications Letters*, vol. 9, no. 8, pp. 1196–1200, 2020.

[9] Z. Fu, Y. Liu, and Y. Yan, "Fast Reconstruction and Iterative Updating of Spatial Covariance Matrix for DOA Estimation in Hybrid Massive MIMO," *IEEE Access*, vol. 8, pp. 213206–213214, 2020.

[10] Y. Liu, Y. Yan, L. You, W. Wang, and H. Duan, "Spatial Covariance Matrix Reconstruction for DOA Estimation in Hybrid Massive MIMO Systems With Multiple Radio Frequency Chains," *IEEE Transactions on Vehicular Technology*, vol. 70, no. 11, pp. 12185–12190, 2021.

[11] M. Rivas-Costa and C. Mosquera, "A Size-Efficient DFT Codebook Approach for DoA Estimation with Hybrid Arrays," in *2025 IEEE 26th International Workshop on Signal Processing Advances in Wireless Communications (SPAWC)*, 2025.

[12] M. Rivas-Costa and C. Mosquera, "Toward efficient super-resolution in SatCom: DoA estimation with hybrid antenna arrays," *IET Conference Proceedings*, vol. 2025, pp. 90–97, 2025.

[13] M. Rivas-Costa and C. Mosquera, "Efficient DoA Estimation with Hybrid Linear and Rectangular Arrays Using Compact DFT Codebooks," 2025. arXiv 2509.03488.

[14] B. Ottersten, P. Stoica, and R. Roy, "Covariance Matching Estimation Techniques for Array Signal Processing Applications," *Digital Signal Processing*, vol. 8, no. 3, pp. 185–210, 1998.

[15] H. Li, P. Stoica, and J. Li, "Computationally efficient maximum likelihood estimation of structured covariance matrices," *IEEE Transactions on Signal Processing*, vol. 47, no. 5, pp. 1314–1323, 1999.

[16] J. Sheinvald and M. Wax, "Direction finding with fewer receivers via time-varying preprocessing," *IEEE Transactions on Signal Processing*, vol. 47, no. 1, pp. 2–9, 1999.

[17] J. R. Magnus, "Maximum likelihood estimation of the GLS model with unknown parameters in the disturbance covariance matrix," *Journal of econometrics*, vol. 7, no. 3, pp. 281–312, 1978.

[18] D. S. Bernstein, *Matrix Mathematics: Theory, Facts, and Formulas*. Princeton, NJ: Princeton University Press, 2 ed., 2009.

[19] S. Park and R. W. Heath, "Spatial Channel Covariance Estimation for the Hybrid MIMO Architecture: A Compressive Sensing-Based Approach," *IEEE Transactions on Wireless Communications*, vol. 17, no. 12, pp. 8047–8062, 2018.

[20] A. Barthelme and W. Utschick, "DoA Estimation Using Neural Network-Based Covariance Matrix Reconstruction," *IEEE Signal Processing Letters*, vol. 28, pp. 783–787, 2021.

[21] J. Sheinvald, M. Wax, and A. Weiss, "On the achievable localization accuracy of multiple sources at high SNR," *IEEE Transactions on Signal Processing*, vol. 45, no. 7, pp. 1795–1799, 1997.